PERFORMANCE PREDICTION OF NOVEL HIGH EFFICIENCY COAXIAL ROTOR CONFIGURATION WITH DISSIMILAR ROTORS

Rahul Ramanujam
Graduate Student
rahulram@iitk.ac.in

Abhishek
Assistant Professor
abhish@iitk.ac.in

Department of Aerospace Engineering
Indian Institute of Technology Kanpur, India

Abstract

This paper proposes a novel dissimilar coaxial rotor concept with significantly reduced rotor-rotor aerodynamic interaction. The performance of the proposed concept is systematically compared with regular coaxial and conventional single rotor configurations using validated BEMT based analysis for hovering flight condition. The hover performance among different rotor configurations is compared in two different ways: 1) equivalent rotor analysis with each rotor having same blade and disc area, and 2) a baseline main rotor is chosen and the performance of different anti-torque options are compared. The equivalent rotor analysis of dissimilar coaxial rotor predicts higher power consumption for the novel concept when compared to regular coaxial and equivalent single rotor, due to high profile power. The profile power is decreased by up to 50% by reducing the RPM of the anti-torque rotor to 50% of the baseline RPM. The proposed concept with reduced RPM of anti-torque rotor is predicted to consume 10-15% less power than equivalent conventional rotor without any tail rotor. The inclusion of tail rotor power for comparison of the performance of dissimilar rotor as an anti-torque concept shows a power reduction of 7–30% when compared to a single main rotor-tail rotor configuration. The analysis also predicts 10–12% less power consumption for dissimilar coaxial rotor design, when compared to a regular coaxial rotor. Within the scope of simplified analysis performed, the proposed concept appears to be an efficient alternative to conventional tail rotor for hovering flight condition.

1 INTRODUCTION

Helicopters spend a significant amount of their operational life performing hovering flight or loitering at low and moderate speeds. Hover requires more power than low and moderate speed forward flight condition. Therefore, higher hovering efficiency is always a desirable feature for helicopters. The induced power is the major contributor to total power during hover. For conventional helicopters, the hover efficiency can be improved by increasing the blade radius and thereby decreasing the disk loading. However, the blade radius is constrained by the profile power and rotor tip speed requirements. Tail rotor also contributes to around 10%-15% of the total power consumed in hovering flight. The tail rotor power spent to counter the rotor anti-torque is not useful as it is not used to generate useful thrust for lifting weight of the helicopter. Therefore, twin rotor concepts such as tandem, coaxial and synchropter were developed to achieve better hovering efficiency as all the power spent is used to generate useful rotor thrust. In tandem, coaxial and synchropter configurations, the two rotors rotate in opposite directions to balance the torque. Among these, the coaxial rotor concept is very popular and Kamov Design Bureau specializes in manufacturing of wide range of helicopters, suitable for naval service and high-speed operations[1]. The key advantage of this configuration is its compactness. However, the coaxial rotors suffer from interference losses between the top and bottom rotor due to increased power consumption by the lower rotor operating in the wake of the upper rotor. The synchropter concept also suffers with similar interference loss as coaxial. The tandem design has partial interference loss and some power penalty arising due to higher empty weight due to two rotor hubs separated by a significant distance resulting in higher transmission weight and structural weight etc. Therefore, it is not easy to establish which of the above rotor configurations offer higher efficiency in hovering flight.

Kim and Brown[2] developed a systematic approach to compare coaxial and conventional rotor performance. In this work they proposed the construction of equivalent single rotor system with the same disk area, blade geometry, and total number of blades as that of the coaxial rotor system. With this, the geometric differences between the two systems are then limited to only the vertical separation between the rotor blades and their relative direction of rotation. Using this approach, he concluded that the articulated coaxial system consumed marginally less induced power than the equivalent single rotor system. In a more detailed study by the same authors[3], the performance comparison was extended to forward and maneuvering flight cases. The study concluded that for all flight conditions, the coaxial system required less induced power than the

equivalent conventional rotor system. In forward flight, the coaxial configuration showed better performance, particularly at pre-transitional advance ratios. It should be noted that, the equivalent rotor system did not include the power lost for anti-torque, which when included, would strongly favour coaxial configuration as a more efficient vertical lift option compared to conventional helicopter configuration.

There have been efforts towards optimizing the performance of conventional as well as coaxial rotor systems. To enhance the performance of conventional rotor for wide range of operating conditions, the optimization of variable speed and variable geometry rotor concept was carried out by the present authors[4]. In this study, a particle swarm optimization (PSO) technique was used to optimize the blade parameters. The relative order of importance of parameters considered for optimizing main rotor power was identified to be the following: rotor speed, rotor radius, chord, twist and TEP extension. For the forward fight conditions analyzed at weight coefficient (C_w) of 0.0065 the multi-variable optimization (MVO) resulted in an additional 5.4% to 12.2% power reduction compared to the single variable optimization (SVO) for the range of advance ratios between 0.01 to 0.25. The aerodynamic optimization of a coaxial proprotor was done by Leishman and Ananthan[5]. Based on the thrust sharing between upper and lower rotors a new expression for figure of merit for a coaxial rotor was identified. BEMT was used to design an optimum coaxial rotor for minimum rotor losses and maximum figure of merit. Monica and Leishman[6] carried out aerodynamic optimization study of a coaxial rotor in hovering flight using Maryland freewake analysis. The study concluded that for optimal performance of coaxial rotor system the rotor blades used on the two sets of rotors would need to use different blade twist distributions and planforms on each rotor, with the upper rotor of the pair must generally be designed with a higher value of solidity.

With the objective of improving the efficiency of rotary wing vehicles during hovering flight, a new configuration for coaxial rotor system is proposed and studied in this paper. This configuration uses two contra-rotating rotors similar to a coaxial rotor concept, thereby obviating the need for tail rotor and associated power loss. The key difference between the regular coaxial rotor and the current proposed design is the use of rotors with different radii and root-cutouts, which are chosen to minimize interaction losses between the two rotors as shown in Fig. 1. The rotor with longer blade and short radius has root-cutout typical of regular main rotor blades. In the current design, it is responsible for contributing the significant portion of useful thrust and hence would be referred to as the “main rotor”. The second rotor spinning in the direction opposite to the main rotor has root-cutout approximately equal to the radius of main rotor and has shorter blades resembling a “flybar” and is termed as “anti-torque” rotor. The two rotors may be arranged at different heights. As for example, a conceptual design sketch of one possible configuration with main rotor at the bottom and the anti-torque rotor at the top is shown in Fig. 2.

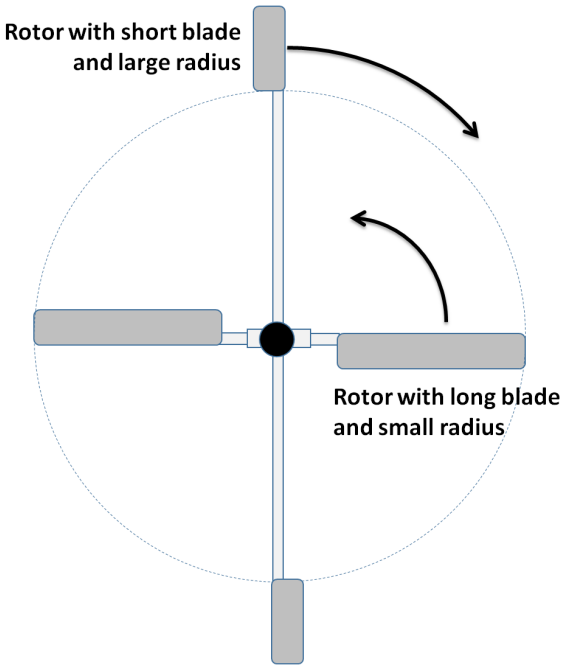

Figure 1: Top view of the proposed dissimilar coaxial contra-rotating rotor concept

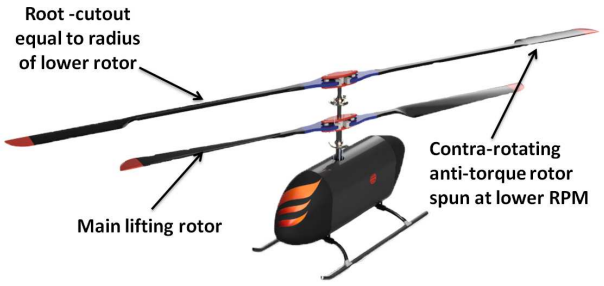

Figure 2: Isometric view showing conceptual helicopter with dissimilar coaxial rotor system

This paper focuses on studying the performance of the novel dissimilar coaxial rotor in hovering flight using BEMT. The hover performance of this design is compared with conventional single rotor and coaxial rotor configurations in the following two ways:

1. The dissimilar coaxial rotor is compared with an equivalent coaxial rotor and a conventional rotor. This approach is similar to that of Kim and Brown[2;3], in which the rotors with same blade area and total disc area are compared for each of the three configurations.

2. The main rotor is kept identical for all three configurations. The use of a tail rotor, a second contra-rotating identical rotor in coaxial configuration and the proposed “flybar” type anti-torque system are com-

pared to identify the most efficient anti-torque system for hovering flight.

In addition, the effect of changing the rotor RPM on the performance of hovering rotor is also established and the possible advantages of the proposed concept over conventional and coaxial concepts are highlighted.

2 ANALYSIS METHODOLOGY

The performance of the proposed dissimilar rotor, conventional single rotor and regular coaxial configurations are compared in hovering flight using Blade Element Momentum Theory (BEMT) based analysis. The flexibility, usability and accuracy of BEMT makes it ideally suited for performance prediction of the different rotor configurations in hovering flight condition. The Blade Element Momentum theory is a mathematical model that combines the basic principles from both Blade Element and Momentum Theory approaches to estimate the non-uniform inflow distribution along the blade.

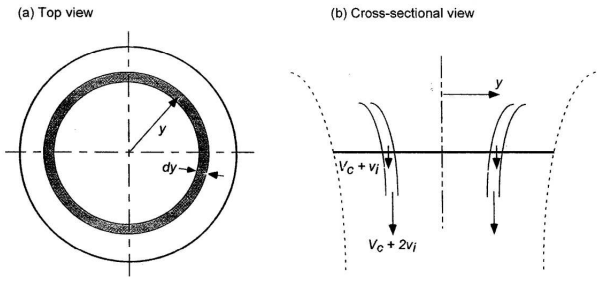

Figure 3: Annulus of rotor disk as used for a local momentum analysis for the hovering rotor

2.1 Blade Element Momentum Theory (BEMT)

The rotor disc area can be discretized in to concentric annuli of radius y and area $dA = 2\pi y dy$ as shown in Fig. 3. Applying one-dimensional momentum theory to a rotor in axial hovering flight, the thrust produced by each annulus is given by:

$$dT = 2\rho v_i^2 dA = 4\pi\rho v_i^2 y dy \tag{1}$$

where ρ is density of air, v_i is induced velocity at the rotor disc. The non-dimensional thrust coefficient is then given by:

$$dC_T = \frac{2\rho v_i^2 dA}{\pi\rho R^2(\Omega R)^2} \tag{2}$$

where C_T is thrust coefficient, R is the radius of the rotor and Ω is the rotational speed of the rotor. The detailed discussion of above theory is available in Leishman[8]. In the non-dimensional form the above equation can be written as:

$$dC_T = 4\lambda^2 r dr \tag{3}$$

where λ is inflow through the rotor. The incremental thrust coefficient of the annulus from blade element theory is:

$$dC_T = \frac{1}{4}\sigma C_{l_\alpha}(\theta r^2 - \lambda r)dr \tag{4}$$

where $\sigma(=\frac{N_b c}{\pi R})$ is the rotor solidity with N_b number of blades with chord length c, C_{l_α} is lift curve slope, θ is collective pitch angle and r is non-dimensional radial station along the blade.

We now equate the two results from Eqs. 3 and 4:

$$\frac{1}{2}\sigma C_{l_\alpha}(\theta r^2 - \lambda r)dr = 4\lambda^2 r dr \tag{5}$$

$$\Rightarrow \lambda^2 + \frac{\sigma C_{l_\alpha}}{8}\lambda - \frac{\sigma C_{l_\alpha}}{8}\theta r = 0 \tag{6}$$

The positive root to solution of the quadratic equation above gives the desired non-linear inflow distribution as:

$$\lambda(r) = \frac{\sigma C_{l_\alpha}}{16}\left[\sqrt{1 + \frac{32\theta r}{\sigma C_{l_\alpha}}} - 1\right] \tag{7}$$

2.2 Prandtl's Tip Loss Factor

The loss of lift near the tips resulting from the induced effects associated with finite length of blades has not been modelled. Prandtl provided a solution to the problem of loss of lift by including a correction factor F in the induced velocity, given by

$$F(r) = \frac{2}{\pi}\cos^{-1}(e^{-f}) \tag{8}$$

where f is given in terms of number of blades (N_b) and radial position on blade: $f(r) = \frac{N_b}{2}\left(\frac{1-r}{\lambda}\right)$ and ϕ is induced inflow angle ($=\frac{\lambda}{r}$). Prandtls F function increases the induced velocity at the tip and reduces the lift generated there. For hovering flight Eq. 7 is modified by using Prandtl's tip loss factor as:

$$\lambda(r) = \frac{\sigma C_{l_\alpha}}{16F}\left[\sqrt{1 + \frac{32F\theta r}{\sigma C_{l_\alpha}}} - 1\right] \tag{9}$$

The iterative process used to calculate λ and F is initiated by assuming $F = 1$ and then calculate $F(r)$ and then λ again in the following steps:

1. Solve for λ with $F = 1$ (no tip loss) using Eq. 9.
2. Calculate F using λ above and $f(r)$ as given below:

$$F(r) = \frac{2}{\pi}\cos^{-1}(e^{-f})$$

$$f(r) = \frac{N_b}{2}\left(\frac{1-r}{\lambda(r)}\right)$$

3. Recalculate $\lambda(r)$ using Eq. 9.
4. Recompute F using expressions above.
5. Recompute $\lambda(r)$
6. Iterate till convergence.

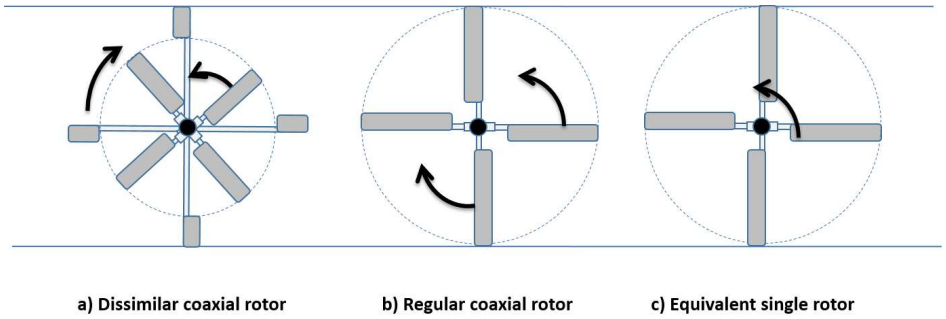

Figure 4: Geometry of dissimilar coaxial, coaxial and conventional rotors used for comparing performance of various equivalent rotor configurations

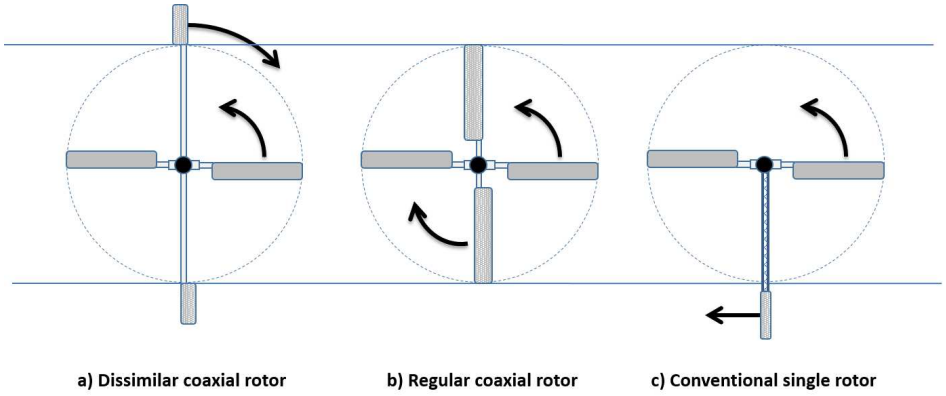

Figure 5: Geometry of dissimilar coaxial, coaxial and conventional rotors used for comparing performance of different anti-torque concepts

3 ROTOR DESCRIPTION

The proposed dissimilar rotor concept aims at improving the efficiency of a hovering rotor by minimizing the interference between the two rotors in a coaxial system. It is achieved by either placing the larger rotor at the top or at the bottom. Due to this arrangement there is minimal or no interaction between the two rotors as the downwash from the larger anti-torque rotor is out of the main rotor disc area. In this arrangement both rotors act as if working as independent rotor thereby giving maximum efficiency without compromising the compactness. The anti-torque rotor counters the main rotor torque and also contributes to total thrust. The profile power for the larger anti-torque rotor can be minimized by operating the anti-torque rotor at lower RPM than the main rotor. Control arrangement for the proposed dissimilar coaxial rotor system is similar to that of regular coaxial rotor system (separate collective pitch control for both rotors and identical cyclic pitch controls). A physical embodiment of this concept may have rotors driven by either two separate engines or motors to allow for different rotational speed. Alternatively, the rotors may be driven by a single motor or engine at different RPMs related by a fixed ratio by use of a mechanical transmission.

As discussed earlier, the dissimilar coaxial rotor concept is compared to the regular coaxial and conventional rotors in two different ways. The first approach is identical to that followed by Kim and Brown[2;3]. In this, equivalent single rotor and coaxial rotor systems are constructed with the same disk area, blade geometry and total number of blades as that of the dissimilar coaxial rotor system. With this, the geometric differences between the three systems are then limited to only the vertical separation between the rotor blades and their relative direction of rotation. The speed of rotation is kept identical for each of the three rotors. A schematic comparing these rotor configurations is shown in Fig. 4. The rotor properties used for this comparison are included in Table 1.

In the second approach, a common main rotor is identified for the three configurations. Different anti-torque configurations are then compared by using a tail rotor for conventional, a second identical contra-rotating rotor for the coaxial configuration and the proposed “flybar” type coaxial dissimilar rotor. The corresponding comparison of these rotor concepts is shown in Fig. 5. The rotor parameters used for comparing the performance of different anti-torque systems are given in Table 2.

It should be noted that the current simple analysis does not model the rotor wake interaction in any manner, however, care is taken to account for possible losses due to presence of tip vortices using Prandtl’s tip loss function and effective blade radius approach for the root vortices present at inboard section of the anti-torque rotor. Further, the large

root cut-out is modeled as an ellipse with major axis four times that of the minor axis. The drag coefficient of the large root cut-out of elliptic shape (rod) is considered as a function of Mach number[7].

Table 1: Rotor properties used for comparison of performance using equivalent rotor approach

Regular coaxial	
Number of rotors	2
Number of blades per rotor	2
Rotor radius (R)	5.5 m
Root cutout	0.133R
Chord	0.4572 m
Twist	0°
Rotor RPM	286.5
Conventional single rotor	
Number of rotors	1
Number of blades per rotor	4
Rotor radius (R)	5.5 m
Root cutout	0.133R
Chord	0.4572 m
Twist	0°
Rotor RPM	286.5
Dissimilar coaxial	
Number of rotors	2
Number of blades per rotor	4
Rotor 1 (Main rotor)	
Radius (R_1)	3.81 m
Root cutout (e_1)	0.133R_1
Chord (C_1)	0.4572 m
Twist	0°
Rotor RPM	286.5
Rotor 2 (Anti-torque rotor)	
Radius (R_2)	5.5 m
Root cutout (e_2)	4 m
Chord (C_2)	0.4572 m
Twist	0°
Rotor RPM	286.5

Table 2: Rotor properties used for comparison of performance of different anti-torque configurations

Regular coaxial	
Number of rotors	2
Number of blades per rotor	2
Rotor radius (R)	3.81 m
Root cutout	0.133R
Chord	0.4572 m
Twist	0°
Rotor RPM	286.5
Conventional single rotor	
Number of rotors	1
Number of blades per rotor	2
Rotor radius (R)	3.81 m
Root cutout	0.133R
Chord	0.4572 m
Twist	0°
Rotor RPM	286.5
Dissimilar coaxial	
Number of rotors	2
Number of blades per rotor	2
Rotor 1 (Main rotor)	
Radius (R_1)	3.81 m
Root cutout (e_1)	0.133R_1
Chord (C_1)	0.4572 m
Twist	0°
Rotor RPM	286.5
Rotor 2 (Anti-torque rotor)	
Radius (R_2)	5.5 m
Root cutout (e_2)	4 m
Chord (C_2)	0.4572 m
Twist	0°
Rotor RPM	143.2

4 RESULTS

The results based on BEMT analysis are discussed in this section. First, the BEMT analysis developed for single and coaxial rotors is validated using the experimental data available in literature. Next, the performance of current design, equivalent single rotor and equivalent coaxial rotor configurations is systematically compared by plotting the power coefficient (C_P) vs. thrust coefficient (C_T). Next, the rotor performance is compared for a complete hovering helicopter system with anti-torque system. For this, the main lifting rotor is kept identical and the anti-torque devices are changed to compare their performance. Finally, some pointers are presented to enhance the efficiency of the proposed dissimilar coaxial rotor.

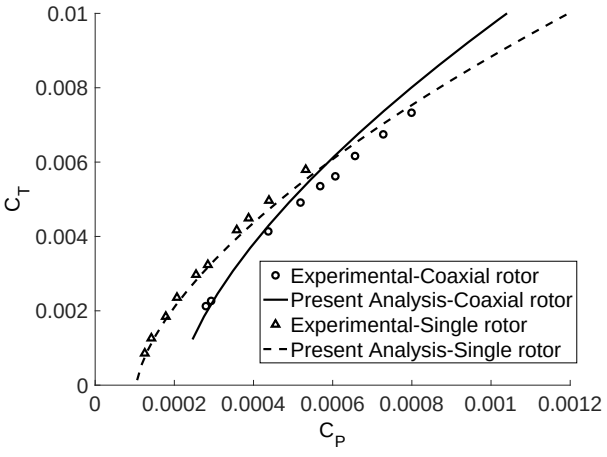

Figure 6: Experimental and predicted rotor thrust vs. power for Harrington rotor 2; experimental results are taken from Ref. 9

4.1 Validation

Harrigtons experimental data[9] for coaxial rotor is used to validate the computational model. The Harrington's rotor 2 with constant chord along the blade is simulated using the BEMT analysis developed. The airfoil lift coefficient of 5.73 is used for the validation results and is retained for all the predictions in this paper. The drag polar used for estimating sectional drag is: $C_d = 0.01 + 0.021\alpha + 0.65\alpha^2$, where α is the local angle of attack at the blade element. The variation of predicted thrust and power coefficient for single and coaxial rotor configurations of Harrington's rotor 2 are shown in Fig. 6. The present analysis shows good correlation with the experimental data for both single and coaxial rotors. This analysis would now be used for predicting the performance of dissimilar coaxial rotor.

4.2 Equivalent Rotor Based Performance Comparison

Performance comparison of the three different rotor configurations is analyzed by taking appropriate equivalence (discussed earlier) into account. The baseline radius of the rotors used for equivalent rotor analysis is 5.5 m. In this section, the physical quantities in equivalent rotor analysis are non-dimenzionalized using radius of 5.5 m and RPM of 286.5. The main rotor and anti-torque rotor of the dissimilar coaxial rotor are spun at the same RPM.

Figure 7(a) compares the predicted C_T vs. total C_P of dissimilar coaxial rotor with single rotor and regular coaxial concepts using equivalent rotor approach. At low thrust conditions ($0.003 < C_T < 0.004$), the regular coaxial rotor and equivalent single rotor consume approximately same power for generating desired thrust. As thrust increases the equivalent single rotor consumes more power than regular coaxial. This observation is similar to that made by Kim and Brown[2] about equivalent single rotor and regular coaxial rotor. The novel dissimilar coaxial rotor appears to be consuming significantly more power than regular coaxial rotor at all thrust conditions. The induced power consumed by each of the three concepts is compared in Fig. 7(b). The regular coaxial rotor consumes the least induced power resulting in least total power among the three candidates. The equivalent single rotor has lower induced power than the dissimilar coaxial rotor, but higher induced power than the regular coaxial. This is possibly because the equivalent dissimilar coaxial rotor has been created by distributing the blade area of each individual blade in to two shorter blades. Each of these short blades have higher losses due to the fact that the tip loss effect (representative of tip vortex presence) has to be included twice for each blade in the analysis, and in addition, root loss effect is also there for the anti-torque rotor due to abnormally large root cutout. These multiple losses result in reduced thrust for the same blade pitch angle for the dissimilar coaxial rotor.

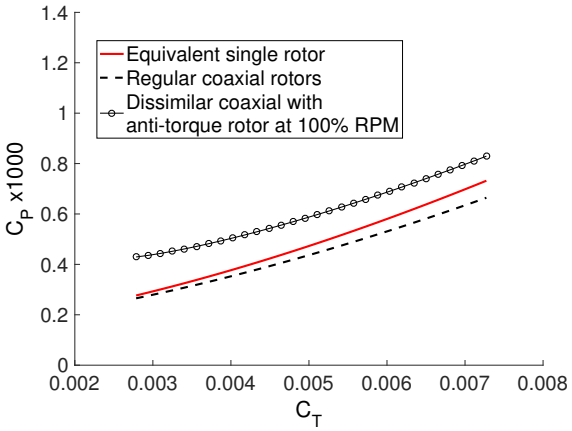

(a) Total power

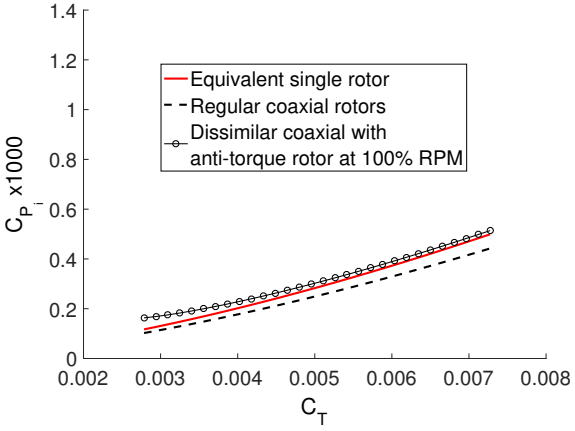

(b) Induced power

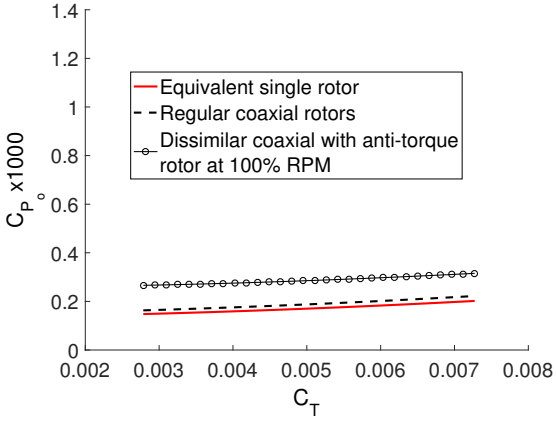

(c) Profile power

Figure 7: Performance comparison of dissimilar coaxial rotor with conventional single rotor and regular coaxial configurations using equivalent rotor concept

Therefore, to generate the same thrust as that of the other two configurations, the blades need to be operated at higher pitch angle and hence higher drag, resulting in significantly increased profile power which penalizes this concept significantly as shown in Fig. 7(c).

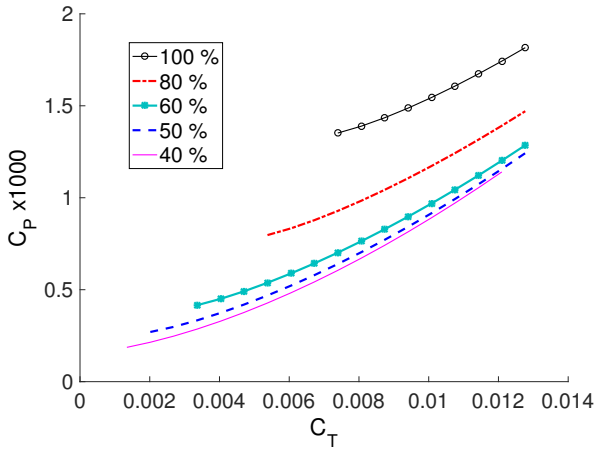

(a) Total power

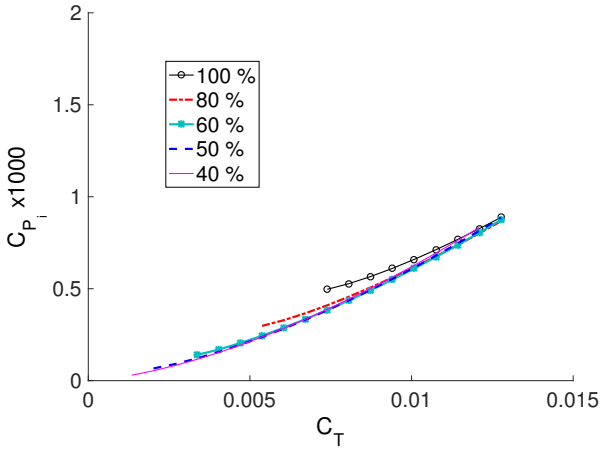

(b) Induced power

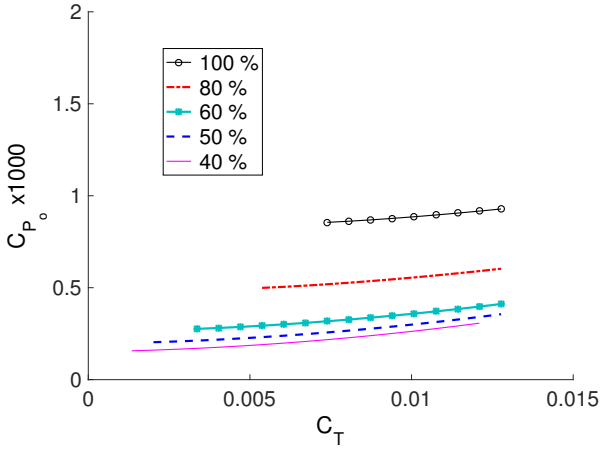

(c) Profile power

Figure 8: Effect of changing RPM of anti-torque rotor on power of dissimilar coaxial rotor

4.3 Effect of Anti-torque Rotor Speed on Rotor Performance

The dissimilar coaxial rotor performed poorly in comparison to single rotor and regular coaxial rotors due to significantly high profile power. To reduce the profile power of the anti-torque rotor, the effect of varying rotor speed (RPM) on the total power and individual power components is systematically studied. In order to have consistent comparison, all the physical quantities in this section are non-dimensionalized by using the physical data for the baseline main rotor of radius 3.81 m and RPM of 286.5 which are kept constant. The baseline properties of the anti-torque rotor are as given in Table 2. In this section, the RPM of the anti-torque rotor is varied from 100% to 40%.

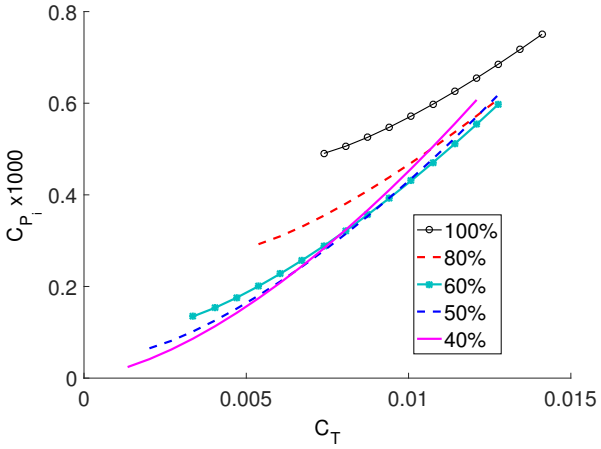

(a) Induced power of main rotor

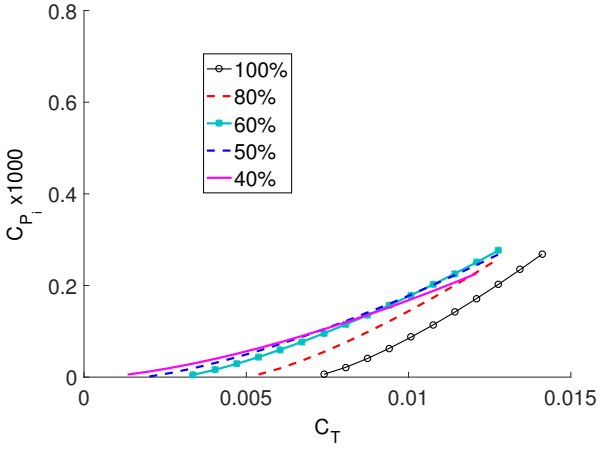

(b) Induced power of anti-torque rotor

Figure 9: Effect of RPM of anti-torque rotor on induced power of dissimilar coaxial rotor

The reduction in the speed of anti-torque rotor from baseline (100% RPM) seems to have significant impact on the total power of the dissimilar coaxial rotor system, as shown in Fig. 8(a). There is dramatic reduction in total power for a given thrust, e.g., for thrust coefficient of 0.0074, total power coefficient reduces by nearly 50%. This dramatic reduction in total power is due to approximately 20% reduction in induced power of rotor system as shown in Fig. 8(b). At higher thrust (such as C_T of 0.01) the reduction in rotor power is nearly 40% and is entirely due to reduction in profile power as the rediction in induced power at higher

C_T is less significant. The variation of profile power with RPM of anti-torque rotor is shown in Fig. 8(c). There is dramatic change in profile power of the rotor system with the reduction in RPM. To understand these variations, it is essential to compare the contribution from each rotor to the individual power components. Figure 9 shows the variation in profile power of main and anti-torque rotors with change in the RPM of anti-torque rotors. The variation of induced power for main rotor is shown in Fig. 9(a). It is observed that the induced power contributed by the main rotor for a given total rotor thrust decreased with RPM of the anti-torque rotor. The reverse is observed for the anti-torque rotor, for which the reduction in RPM results in increase in induced power as shown in Fig. 9(b).

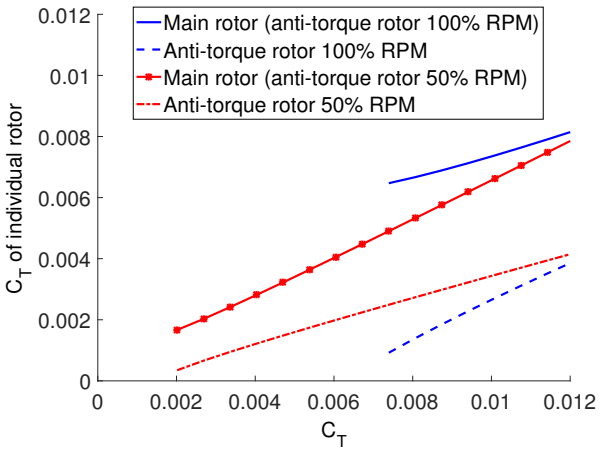

(a) C_T distribution between rotors

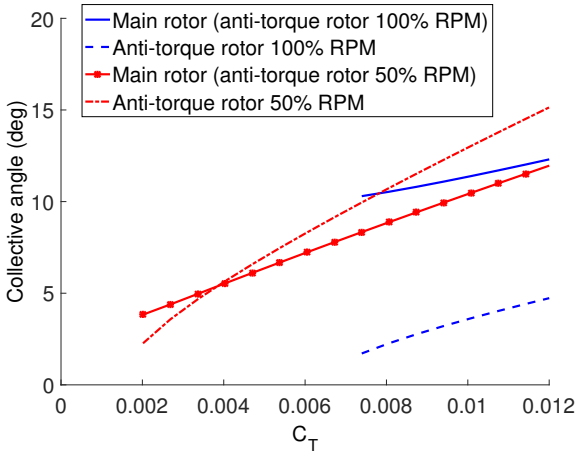

(b) Collective angle

Figure 10: Effect of RPM of anti-torque rotor on profile power of dissimilar coaxial rotor

The reduction in induced power of main rotor and increase in induced power of anti-torque rotor is due to redistribution of the thrust share between both the rotors for a given thrust as shown in Fig. 10(a). This happens due to the requirement to balance the torque from both the rotors. The contribution of main rotor thrust to total thrust decreases with RPM and contribution of anti-torque rotor increases with RPM. The corresponding variation of collective angle for both the rotors for different total rotor thrust is shown in Fig. 10(b) which explains the corresponding change in thrust contribution.

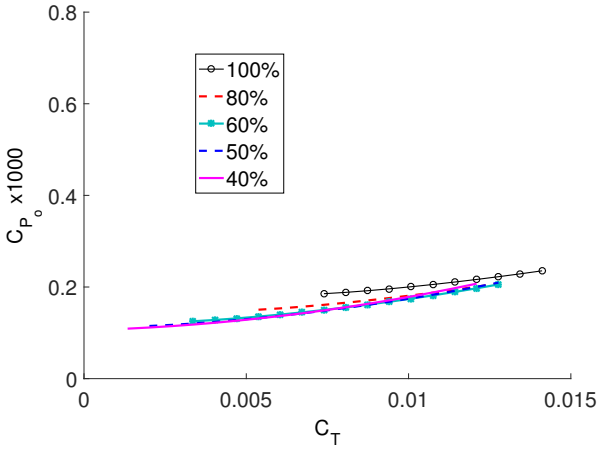

(a) Profile power of main rotor

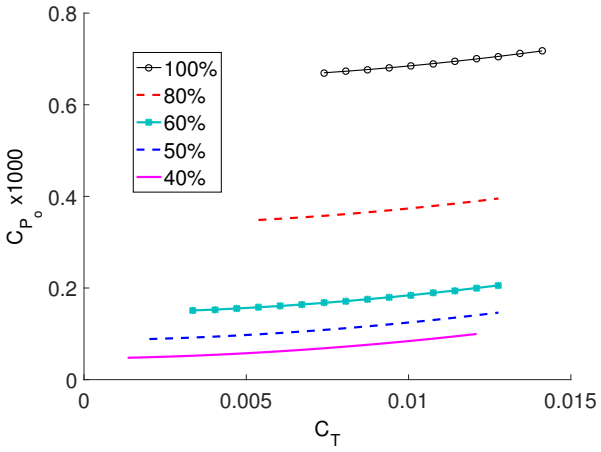

(b) Profile power of anti-torque rotor

Figure 11: Effect of RPM of anti-torque rotor on profile power of dissimilar coaxial rotor

The variation of profile power of main rotor with RPM of anti-torque rotor is shown in Fig. 11(a). The change in profile power is less significant as the change in drag due to redistribution of thrust between main and anti-torque rotors is small. The dramatic reduction in profile power of the anti-torque rotor with reduction in RPM is shown in Fig. 11(b). This reduction is primarily due to reduction in drag of the lifting area as well as the large blade support rod with reduced tip speed.

Overall, it is observed that the total rotor power decreases with reduction in RPM of anti-torque rotor for low thrust ranges. From the current analysis, 50% of the baseline RPM of the main rotor may be taken as the optimum rotor RPM of the anti-torque rotor. Going to any lower RPM would mean that the blades of anti-torque rotor may have to operate at very high angles of attack resulting in stall. Since

the anti-torque rotor is placed outside the main rotor disc area, the rotor radius of anti-torque rotor is large. Because of large radius, a lower RPM is sufficient to generate adequate drag in the anti-torque rotor blade section to balance the torque of the main rotor. It should be noted that for the baseline RPM case, the minimum C_T achieved by the main rotor to ensure torque equilibrium is 0.007 approximately, this is due to the fact that the anti-torque rotor is already operating at its minimum thrust condition.

4.4 Equivalent Rotor Based Performance Comparison with Reduced RPM

The equivalent rotor comparison performed earlier is now repeated with RPM of the anti-torque rotor reduced to 50% of the baseline, all other things remaining the same. The variation of total power, induced power and profile power with the total C_T for the three concepts are shown in Figs. 12(a), 12(b) and 12(c) respectively. The dissimilar coaxial is now performing marginally better than the regular coaxial, especially at low to moderate C_T values. It also shows lower power consumption than the conventional equivalent rotor due to lower profile power as induced power for the conventional and dissimilar coaxial are nearly identical. At $C_T > 0.0065$ the two rotor configurations require nearly same power. The induced power for the regular coaxial continues to be the lowest among the configurations compared. The reduction in the total power of the dissimilar coaxial is primarily due to significant reduction in the profile power. The percent reduction in the total power of the dissimilar coaxial rotor due to the reduction of the RPM of the anti-torque rotor for various C_T is shown in Fig. 13. The power reduction is as high as 40% for $C_T = 0.004$ and reduces to nearly 20% for $C_T = 0.0073$. This decrease is possibly due to the fact that at lower RPM, the anti-torque rotor has to operate at larger angle of attack which increases profile power again due to increased drag predicted by the drag polar used in present analysis.

It appears that in the equivalent rotor approach the performance of dissimilar coaxial rotor concept is penalized as the given rotor blade is split into blades with smaller span, thereby increasing the induced losses of the blade. Therefore, the performance of the proposed design is studied from the perspective of an anti-torque system in the next section.

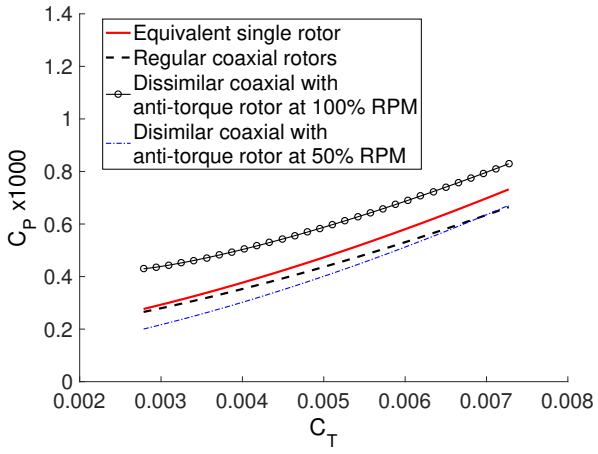

(a) Total power

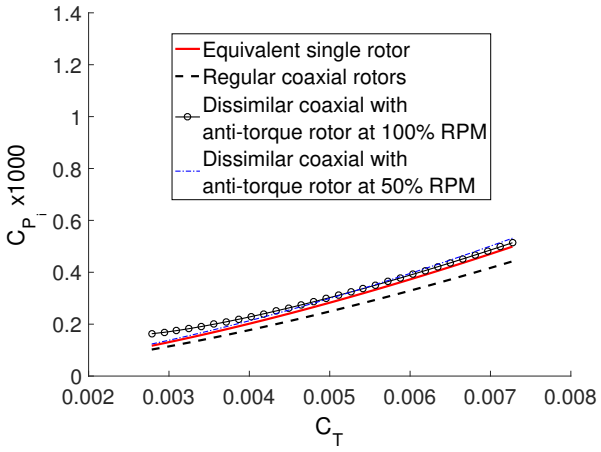

(b) Induced power

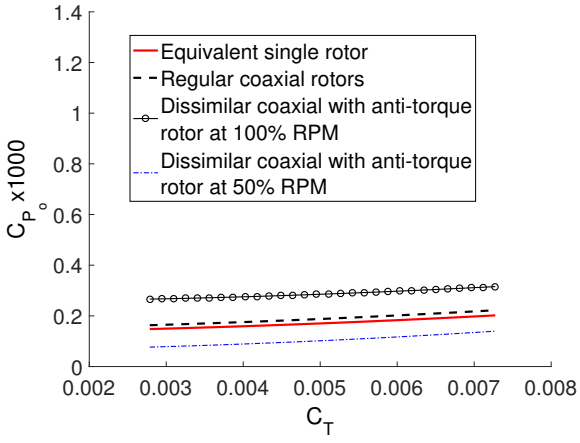

(c) Profile power

Figure 12: Performance comparison of dissimilar coaxial rotor with conventional single rotor and regular coaxial configurations using equivalent rotor concept with anti-torque rotor operating at 50% RPM

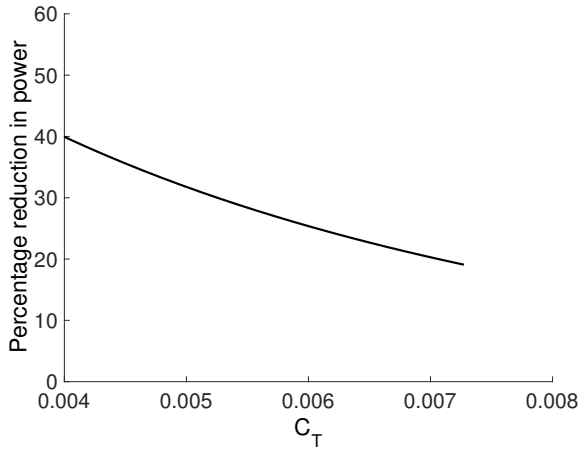

Figure 13: Percent power reduction for dissimilar coaxial rotor with anti-torque rotor RPM reduced to 50% RPM of the baseline

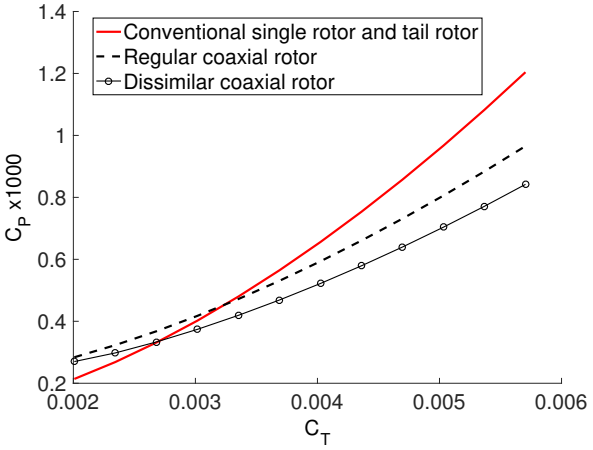

Figure 14: Performance comparison of anti-torque mechanism efficiency of dissimilar coaxial rotor with existing rotorcraft designs

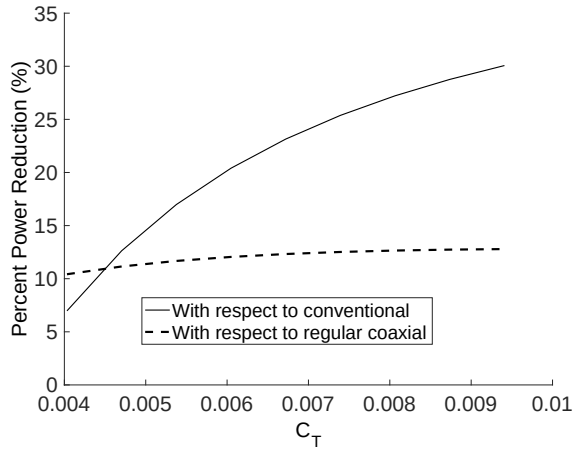

Figure 15: Percentage power reduction for dissimilar coaxial rotor when compared to conventional single rotor and regular coaxial rotor

4.5 Comparison of Performance of Various Anti-torque Concepts

The efficiency of the dissimilar coaxial rotor system as an anti-torque device over existing anti-torque mechanisms is compared with regular coaxial rotor and conventional single rotor and tail rotor setup. In this case, the total power for the conventional rotor also includes the tail rotor power, which was not considered in the equivalent rotor analysis. All the physical quantities in this section are non-dimensionalized by using the physical data for the baseline rotor of radius 3.81 m and RPM of 286.5. To ensure that the torque is balanced for the conventional single rotor analysis, the tail rotor power is also included in total power and is assumed to be 10% of the total main rotor power in hover, as suggested in Refs. 2 and 8.

A regular coaxial rotor has two contra rotating baseline rotors placed one above the other. The simulation is carried out for torque equilibrium, the total thrust and power from both the rotors are added to obtain total thrust and power. Dissimlar coaxial rotor uses the baseline rotor as main rotor and the anti-torque rotor is placed outside the main rotor area and is spun at 50% of the RPM of the main rotor. The power variation with rotorcraft thrust for the three anti-torque concepts is compared in Fig. 14. All the configurations has the same main rotor radius and rotor RPM. It is observed that for $C_T > 0.003$, the dissimilar coaxial rotor consumes least total power for the same rotor thrust compared to the regular coaxial rotor and conventional single main rotor-tail rotor configurations. Superiority of dissimilar coaxial rotor over regular coaxial rotor and conventional single rotor configurations is quantitatively shown in the Fig. 15. Dissimilar coaxial rotor consistently consumes 11–13% less power, when compared to regular coaxial rotor for the range of thrust coefficients analyzed. It consumes 7%–30% less power compared to conventional single rotor as shown in Fig. 15. The high power saving of dissimilar coaxial rotor over conventional single rotor is because of the increase in tail rotor power of the conventional helicopter at high thrust conditions. For a moderate C_T of 0.0067, the dissimilar rotor configuration consumes 23% less power. This is mainly due to the fact that the tail rotor power is wasted in overcoming the torque reaction, without contributing to the useful thrust generation. For the dissimilar coaxial, both the main rotor and anti-torque rotors contribute towards total thrust. In this approach, the regular coaxial rotor is partially penalized because, a second contra-rotating rotor is employed to counter the torque without having to contribute significantly to thrust generation.

The share of thrust contribution of the individual rotors is shown in terms of C_T of individual rotors in Fig. 16(a). The corresponding percent share is shown in Fig. 16(b). It is observed that for $C_T > 0.004$ the anti-torque rotor contributes to approximately 28–35% of total thrust. Typical thrust distribution for total $C_T = 0.0065$ for main rotor and the anti-torque rotor is shown in Fig. 17. The effect of tip loss function can be clearly seen for both the rotors. The

power share of the main rotor and anti-torque rotor is shown in Fig. 18. The anti-torque rotor contributes to 33.3% and the main rotor requires 66.7% power of the total power consumed by the rotor for all thrust conditions. This is due to the fact that both the rotors are trimmed for equal torque and the RPM of the anti-torque rotor is 50% of the main rotor. The power distribution for main rotor and anti-torque rotors for $C_T = 0.0065$ is shown in Fig. 19.

The anti-torque rotor has large root-cutout, which contributes to only the profile power component of the anti-torque rotor. The power share of the bluff-body attachment between the blade and the hub and the aerodynamic portion of the anti-torque rotor is shown in Fig. 20. It is observed that at moderate thrust of 0.0067, the blade attachment accounts for approximately 25% of the total power of the anti-torque rotor and the lifting portion accounts for remaining 75%. Since, the rotational speed of the anti-torque rotor remains constant, the blade attachment consumes constant power irrespective of the rotor thrust.

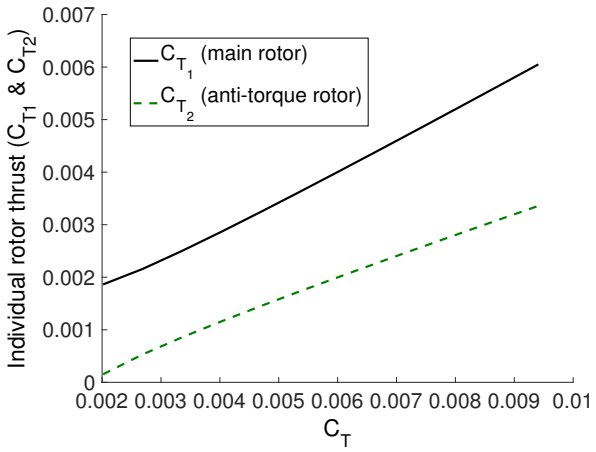

(a) Thrust share of individual rotors

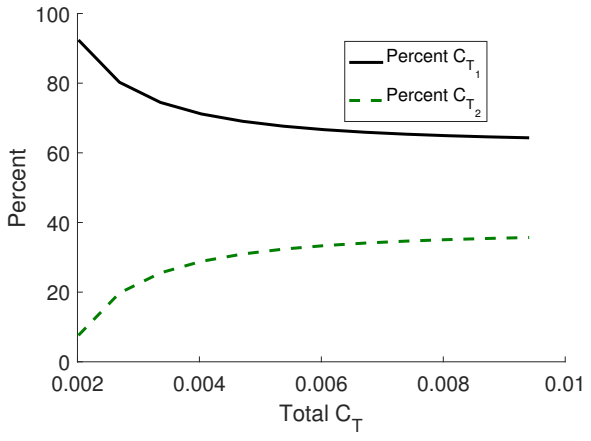

(b) Percent thrust share

Figure 16: Thrust share of main and anti-torque rotor as a function of total thrust

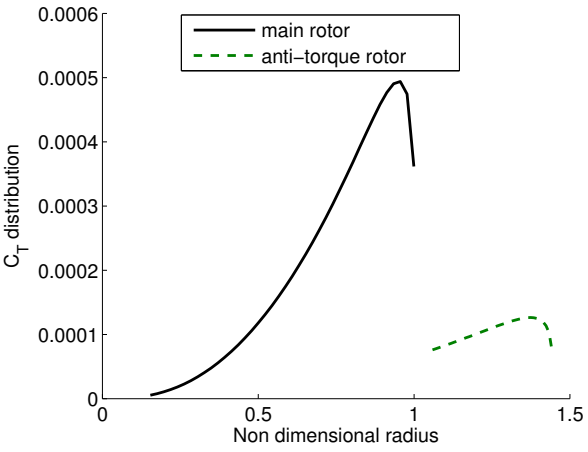

Figure 17: Thrust distribution of main rotor and anti-torque rotor for $C_T = 0.0065$

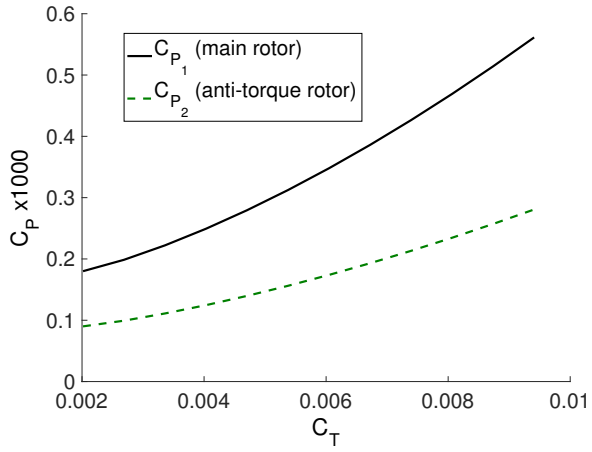

Figure 18: Power share of main rotor and anti-torque rotor

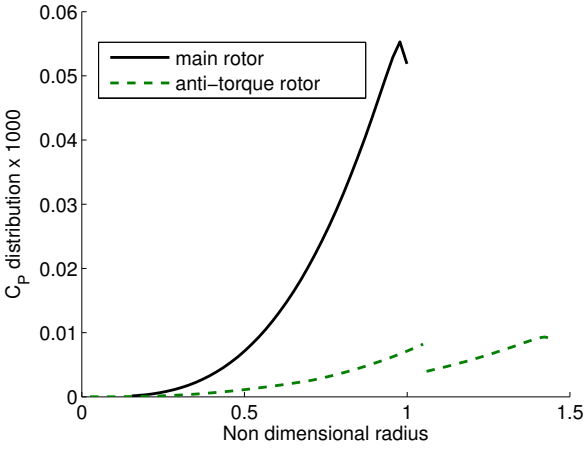

Figure 19: Power distribution of main rotor and anti-torque rotor for $C_T = 0.0065$

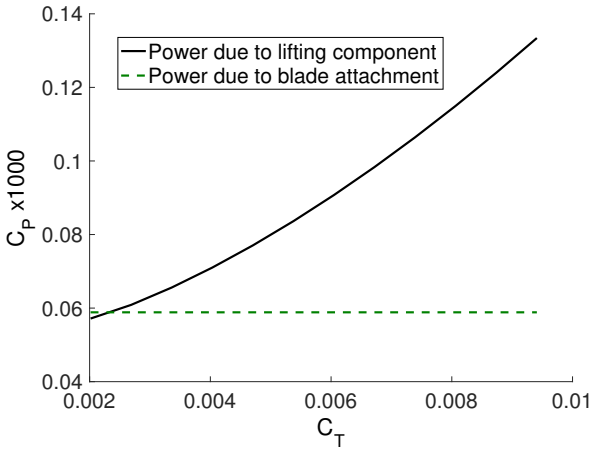

Figure 20: Power share of blade hub attachment and blade lifting section for anti-torque rotor power

5 FUTURE WORK

The analysis has currently been carried out only for the hover flight condition and it would be extended to forward flight in future work. Further, the observations made in this paper would be experimentally verfied for small scale rotor blades by constructing a coaxial rotor test stand to understand the rotor wake interactions in detail. The effect of positioning the anti-torque rotor with respect to the main rotor can also be studied.

6 CONCLUSIONS

This paper proposes a novel coaxial rotor concept which makes use of dissimilar rotors. The proposed concept is analyzed for hovering flight using BEMT and its performance was compared with single main rotor and regular coaxial rotor configurations. For this two approaches were employed: 1) equivalent rotor analysis was carried out, in which each configuration has same blade and disc area and 2) a baseline main rotor was selected and the performance in the presence of different anti-torque concepts is compared. Based on this analysis, the following key conclusions can be drawn:

1. Equivalent rotor analysis of dissimilar coaxial rotor predicts higher power consumption for the novel concept when compared to regular coaxial and equivalent single rotor, due to high profile power. The profile power is reduced dramatically by decreasing the RPM of the anti-torque rotor. Based on RPM sweep study, setting the RPM of anti-torque rotor to 50% of the baseline main rotor RPM gives favourable result. With this RPM, the dissimilar rotor concept is predicted to consume 2-6% less power than the regular coaxial rotor and 10-15% less power than equivalent conventional.

2. The comparison of the performance of dissimilar rotor as an anti-torque concept shows a power reduction of 7–30% when compared to a single main rotor-tail rotor configuration. The analysis also predicts 10–12% less power consumption for dissimilar coaxial rotor design, when compared to a regular coaxial rotor.

3. With appropriate choice of anti-torque rotor length (0.44R of main rotor for present analysis), it can contribute 28-35% of total thrust while requiring only 33% of total power. The slowing down of the anti-torque rotor may also enable forward flight at higher speeds without the onset of the advancing blade transonic effects. This needs to established through further studies.

4. Although the current study is simple and the trends observed may be qualitative at best, the proposed concept appears to be a promising alternative and an efficient replacement for conventional tail rotor for hovering flight. The proposed concept would result in relative compact design as it would not require long tail boom for supporting tail rotor. The superiority of this concept when compared to a coaxial rotor may need further detailed analysis and experimentation.

References

[1] Wikipedia Article, "Kamov", *URL: https://en.wikipedia.org/wiki/Kamov* as retreived on 22 July 2017.

[2] Kim, H. W., and Brown, R.E., "A Rational Approach to Comparing the Performance of Coaxial and Conventional Rotors," *Journal of the American Helicopter Society*, Vol. 55, No. 1, 2010, pp. 012003-1–012003-9.

[3] Kim, H. W., and Brown, R.E., "A Comparison of Coaxial and Conventional Rotor Performance," *Journal of the American Helicopter Society*, Vol. 55, No. 1, 2010, pp. 012004-1–012004-20.

[4] Ramanujam, R., and Abhishek, A., Performance optimization of a variable speed and variable geometry rotor concept, *Journal of Aircraft*, Vol. 54, No. 2, March 2017, pp. 476–489. doi: 10.2514/1.C033869

[5] Leishman, J. G., and Ananthan, S., Aerodynamic Optimization of a Coaxial Proprotor, Proceedings of the 62nd Annual Forum of the American Helicopter Society International, Phoenix, AZ, May 911, 2006.

[6] Leishman, J. G., and Ananthan, S., Aerodynamic Optimization Study of a Coaxial Rotor in Hovering Flight, *Journal of the American Helicopter Society*, Vol. 57, No. 4, 2012, pp. 042003-1–042003-15.

[7] Munson, B. R., Young, D. F., and Okiishi, T. H., "Fundamentals of Fluid Mechanics," 4th ed., Hoboken, NJ: J. Wiley & Sons, 2006.

[8] Leishman, J. G., "Principles of Helicopter Aerodynamics," 2nd ed., Cambridge University Press, New York, NY, 2006.

[9] Harrington, R. D.," Full-Scale-Tunnel Investigation of the Static Thrust Performance of a Coaxial Helicopter Rotor," NACA TN-2318, March 1951.